# Highly Dispersive Spin Excitations in the Chain Cuprate $Li_2CuO_2$

W.E.A. Lorenz[1] [(a)], R.O. Kuzian[1,2], S.-L. Drechsler[1], W.-D. Stein[3], N. Wizent[1], G. Behr[1], J. Málek[1,7], U. Nitzsche[1], H. Rosner[6], A. Hiess[4], W. Schmidt[5], R. Klingeler[1], M. Loewenhaupt[3] and B. Büchner[1]

[1] *Leibniz-Institut für Festkörper- und Werkstoffforschung (IFW) Dresden, Germany*
[2] *Institute for Problems of Materials Science Krzhizhanovskogo 3, 03180 Kiev, Ukraine*
[3] *Institut für Festkörperphysik, Technische Universität Dresden, 01062 Dresden, Germany*
[4] *Institut Laue Langevin, F-38042 Grenoble Cedex 9, France*
[5] *Jülich Centre for Neutron Science JCNS, Jülich, Germany*
[6] *Max-Planck-Institut für Chemische Physik fester Stoffe, Dresden, Germany*
[7] *Institute of Physics, ASCR, Prague, Czech Republic*



PACS 74.72.Jt – Other cuprates
PACS 78.70.Nx – Neutron inelastic scattering
PACS 75.30.Ds – Spin waves

**Abstract.** - We present an inelastic neutron scattering investigation of $Li_2CuO_2$ detecting the long sought quasi-1D magnetic excitations with a large dispersion along the $CuO_2$-chains studied up to 25 meV. The total dispersion is governed by a surprisingly large ferromagnetic (FM) nearest-neighbor exchange integral $J_1 = -228$ K. An anomalous quartic dispersion near the zone center and a pronounced minimum near (0,0.11,0.5) r.l.u. (corresponding to a spiral excitation with a pitch angle about 41°) point to the vicinity of a 3D FM-spiral critical point. The leading exchange couplings are obtained applying standard linear spin-wave theory. The $2^{nd}$ neighbor inter-chain interaction suppresses a spiral state and drives the FM in-chain ordering below the Néel temperature. The obtained exchange parameters are in agreement with the results for a realistic five-band extended Hubbard Cu $3d$ O $2p$ model and LSDA+$U$ predictions.

**1. INTRODUCTION.** – $Li_2CuO_2$ is the first [1] and the most frequently studied compound of the growing class of edge-shared spin-chain cuprates [2–7]. Owing to its structural simplicity with ideally planar $CuO_2$ chains (see Fig. 1) it has been considered as a model quasi-one-dimensional (1D) frustrated quantum spin system. In almost all edge-shared cuprate chain compounds the spins are expected to be coupled along the chains via nearest neighbor (NN) ferromagnetic (FM) and next-nearest neighbor (NNN) antiferromagnetic (AFM) exchange interactions, $J_1$ and $J_2$, respectively. Due to the induced frustration FM and spiral in-chain correlations are competing. While in the 1D model the ground state is governed by the ratio $\alpha = -J_2/J_1$, the actual 3D magnetic order sensitively depends on the strength of the inter-chain couplings and anisotropy. In $Li_2CuO_2$, below $T_N \approx 9$ K [8, 9] a long-range collinear commensurate AFM inter-chain with FM in-chain (CC-AFM-FM) magnetic ordering evolves. However, a proper understanding, necessary for a critical evaluation of theoretical studies, especially of

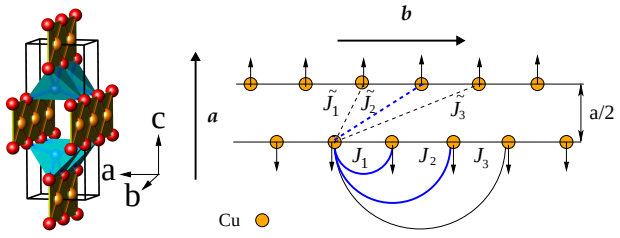


Figure 1: (Color online) Left: The crystallographic structure of $Li_2CuO_2$ comprises two AFM coupled $CuO_2$ spin-chains per unit cell running along the $b$-axis (orange ● – $Cu^{2+}$, red ● – $O^{2-}$, bright blue ● – $Li^+$). The unit cell is indicated by the outer black cuboid. Right: the main intra- and inter-chain exchange paths, $J_1$, $J_2$, and $\tilde{J}_2$ marked by blue arcs and dashed lines, respectively. Notice the frustration introduced by an AFM inter-chain coupling for any non-FM in-chain ordering.

[(a)] E-mail: w.lorenz@ifw-dresden.de

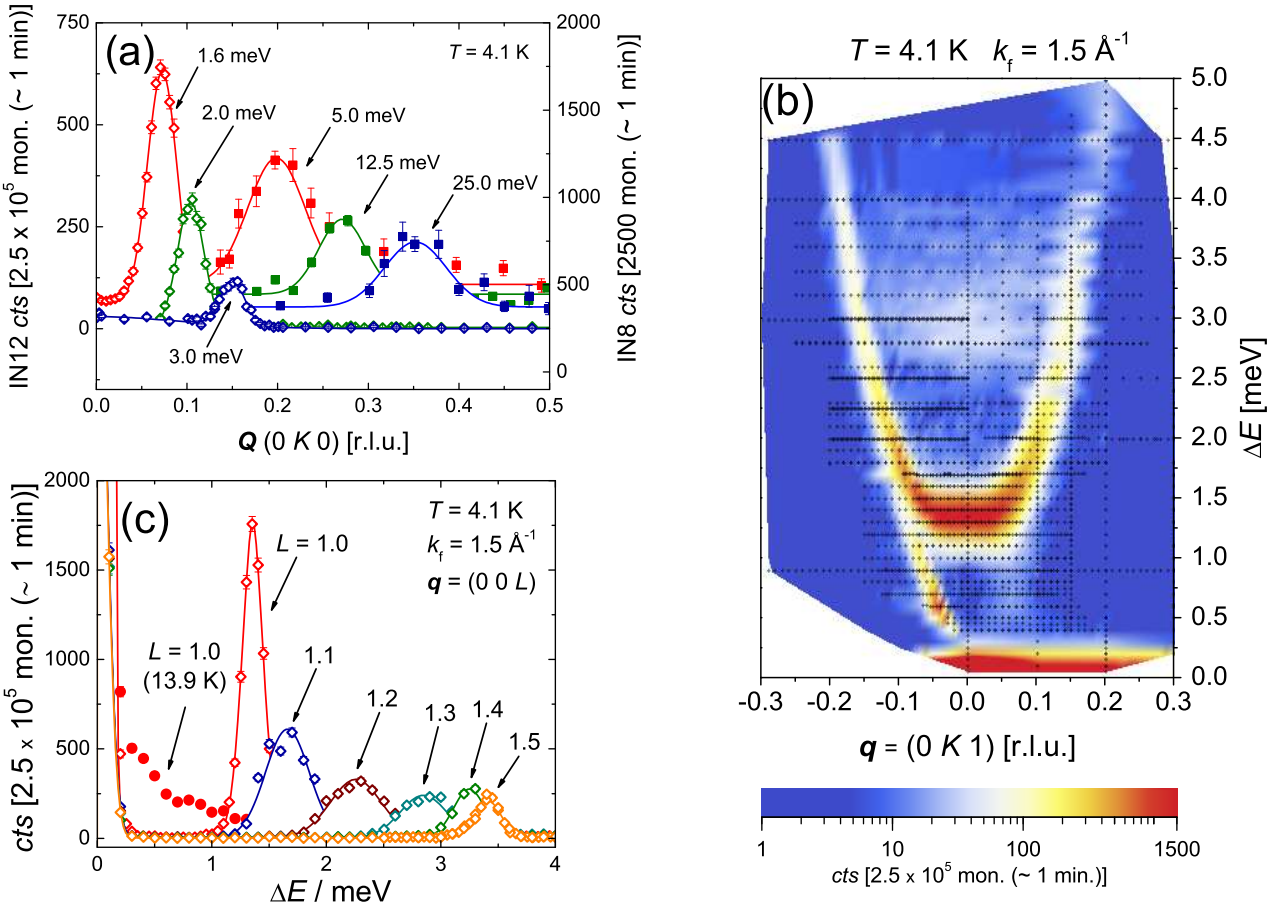


Figure 2: (Color online) (a) Constant energy scans for momentum transfer along the chains with $\mathbf{q} = (0\ K\ 1)$ at IN12 ($\Delta E \leq 3$ meV; open symbols) and $\mathbf{q} = (0\ 1+K\ 0)$ for IN8 data ($\Delta E \geq 5$ meV; filled symbols). (b) Intensity map of the low energy spectrum, interpolated from the IN12 data points (•). The sizeable intensity below the gap energy, i.e. at energy transfer $\lesssim 1$ meV and $q_b$ around -0.05 is a spurious Bragg tail. (c) The dispersion perpendicular to the chains was measured by constant $Q$-scans; lines are Gaussian fits. Filled symbols: the measured intensity at the zone center for $T > T_N$.

electronic/magnetic structure calculations [10–14], is still missing. In particular, this concerns a precisely enough knowledge of the main exchange interactions. The knowledge of realistic values is helpful also for the understanding of related "frustrated ferromagnets" [15, 16] such as $Ca_2Y_2Cu_5O_{10}$ [17], $La_6Ca_8Cu_{24}O_{41}$ [2] with FM in-chain ordering and $LiVCuO_4$, $LiCu_2O_2$ with helimagnetism and multiferroicity, all being of considerable current interest.

A previous inelastic neutron scattering (INS) study aimed to determine the exchange integrals was not conclusive [18]. It revealed an anomalous low-lying branch of hardly dispersive and overdamped spin excitations in chain direction. Its linear spin-wave (LSW) analysis results in unrealistically small in-chain exchange integrals. The missing, but expected, dispersive quasi-1D spin chain excitation remained as a challenging puzzle for the community [10, 11, 19]. In Sec. 3 we present new INS data which unambiguously show the presence of a strongly dispersive in-chain spin mode. The main exchange integrals are derived applying the LSW-theory [20] and in Sec. 4 we compare our results with those of related chain cuprates as well as with predictions of band structure and cluster calculations. A criticism of improper Curie-Weiss analysis of spin susceptibility data is provided and consequences for the direct FM Cu-O exchange parameter $K_{pd}$ entering extended Hubbard models are discussed.

**2. EXPERIMENTAL.** – A single crystal of $^7Li_2CuO_2$ was grown for INS experiments by the travelling solvent floating zone technique under high pressure [21]. In order to avoid vaporization of $Li_2O$ during growth a 4:1 Ar:$O_2$ atmosphere at 50 bar was chosen. A fast growth rate of 10 mm/h inhibits growth of impurity phases. Isotope enriched $^7$Li was employed to avoid the significant neutron absorption coefficient of $^6$Li. The sample was characterized by X-ray powder diffraction, polarized light microscopy, magnetization and specific heat measurements. By X-ray powder diffraction no impurity phase was found. The macroscopic magnetization and specific heat data of the sample agree with literature data, i.e. AFM order is found below $T_N = 9.2$ K and a weak FM component evolves below $T_2 \approx 3$ K [9, 22, 23].

INS experiments were performed with thermal and cold neutrons at the three-axis-spectrometers IN8 and IN12 at the ILL, Grenoble, France. Four single crystals with a total mass of 3.8 g were mounted together in the (0 $K$ $L$) scattering plane with a resulting sample mosaicity of 3°. For both instruments, focusing PG(002) monochromator and analyzer have been utilized. The measurements at IN8 were taken with fixed final momentum $k_{\rm f} = 2.662\,{\rm \AA}^{-1}$ with PG-filter on $k_{\rm f}$. IN12 was configured with $k_{\rm f} = 1.5\,{\rm \AA}^{-1}$ and Be-filter on $k_{\rm f}$. Most scans have been done in the CC-AFM-FM phase at $T = 4.1\,{\rm K}$ well above another not yet well understood magnetic phase below $T_2$ . Anyhow, the observed changes of the INS spectra in this low-$T$ phase (not shown here) are weak.

**3. RESULTS AND DATA ANALYSIS.** – The results of our INS studies are summarized in Fig. 2. Representative spectra of constant energy scans as taken at IN12 and IN8 for moment transfer along the chains ($b^*$) are displayed in Fig. 2(a). The main result is the observation of a highly dispersive excitation which is strong at the magnetic zone center and significantly weakens at higher energies. With the chosen experimental setup the magnetic branch could be traced up to energy transfers of 25 meV. The measured data points along (0 $K$ 1) taken at IN12 with cold neutrons are summarized in the color map Fig. 2(b). Note, that the reflections are periodic with the magnetic unit cell and their strongly reduced intensity above $T_{\rm N}$ observed up to energy transfers of 15 meV does confirm their magnetic nature (see Fig. 2 (c)). At the magnetic zone center (0 0 1), a gap of $\Delta = 1.36\,{\rm meV}$ is observed. The excitations for momentum transfer along (0 0 $1 + L$) are only weakly dispersive in agreement with the results of Ref. [18]. Respective constant $\mathbf{q}$-scans are shown in Fig. 2(c). Note, that the mosaicity of the sample broadens the excitations along $L$ which is less pronounced for moment transfer along $K$ due to the longer $b^*$-axis.

As shown in Fig. 2(b) we observe further inelastic features for moment transfer along the chain. In addition, the data in Fig. 2(b) also exhibit weak and presumably incommensurate (IC) magnetic scattering below the magnon gap energy. The origin of these low-energy excitations is not yet clear and will be addressed in future studies. Furthermore, there is a continuous feature appearing at double the energy of the anisotropy gap which is possibly attributed to two-magnon scattering. We also mention that we have observed low-lying and strongly broadened excitations along $b^*$ similarly as in Ref. [18]. However, the intensity of these excitations was roughly two orders of magnitude weaker than that reported ibidem.

According to ESR measurements [24] the exchange interactions show an uniaxial anisotropy with the easy-axis directed along the crystallographic $a$-axis. We describe the corresponding Cu momenta by the spin-Hamiltonian

$$\hat{H} = \frac{1}{2}\sum_{\mathbf{m},\mathbf{r}}\left[J^z_{\mathbf{r}}\hat{S}^z_{\mathbf{m}}\hat{S}^z_{\mathbf{m+r}} + J^{xy}_{\mathbf{r}}\hat{S}^+_{\mathbf{m}}\hat{S}^-_{\mathbf{m+r}}\right] \qquad (1)$$

where $\mathbf{m}$ enumerates the sites in the magnetic (Cu) lattice, the vector $\mathbf{r}$ connects sites with an exchange coupling $J_{\mathbf{r}}$ [25]. The $z$-axis is taken along the easy-axis, i.e. the $a$-axis. Within the LSW-theory [20], the dispersion-law reads

$$\omega_{\mathbf{q}} \;=\; \sqrt{\left(J^{xy}_{\mathbf{q}} - J^{xy}_{\mathbf{0}} + \tilde{J}^{xy}_{\mathbf{0}} - D\right)^2 - \left(\tilde{J}^{xy}_{\mathbf{q}}\right)^2}, \quad (2)$$

where $J_{\mathbf{q}} \equiv (1/2)\sum_{\mathbf{r}} J_{\mathbf{r}} \exp(\imath\mathbf{qr})$ is the Fourier transform of the in-chain exchange integrals, and analogously for the inter-chain integrals $\tilde{J}_{\mathbf{q}}$. The exchange anisotropy $D \equiv J^z_0 - J^{xy}_0 - \tilde{J}^z_0 + \tilde{J}^{xy}_0$ causes the abovementioned spin gap $\Delta = \omega_{\mathbf{0}}$ in our case (see Fig. 3). Their relation reads

$$\Delta = \sqrt{D\left(D - 2\tilde{J}^{xy}_0\right)}, \quad \text{or} \quad D = \tilde{J}^{xy}_{\mathbf{0}} - \sqrt{\left(\tilde{J}^{xy}_{\mathbf{0}}\right)^2 + \Delta^2}\,. \qquad (3)$$

In the summations over $\mathbf{r}$ we retain only the leading terms (see Fig. 1). According to LSDA+$U$ based magnetic structure calculations they are given by the following in-chain integrals: $J_1$, $J_2$, $J_3$, (corresponding to $\mathbf{r} = \mathbf{b}$, $2\mathbf{b}$, $3\mathbf{b}$ respectively) and inter-chain integrals: $\tilde{J}_{111}$, $\tilde{J}_{131}$, (corresponding to $\mathbf{r}_{111} = (\mathbf{a}+\mathbf{b}+\mathbf{c})/2$, $\mathbf{r}_{131} = (\mathbf{a}+3\mathbf{b}+\mathbf{c})/2$). For $q_a a$ or $q_c c = \pi$ the inter-chain dispersion caused by $\tilde{J}^{xy}_{\mathbf{q}}$ vanishes and Eqn. (2) simplifies:

$$\omega_{\mathbf{q}} = J^{xy}_{\mathbf{q}} - J^{xy}_{\mathbf{0}} + \tilde{J}^{xy}_{\mathbf{0}} - D = J^{xy}_{\mathbf{q}} - J^{xy}_{\mathbf{0}} + \Delta_1, \qquad (4)$$

i.e. the single-chain dispersion can be read off *directly* by subtracting the effective gap $\Delta_1$, only.

Our INS data are well fitted by Gaussian distributions. The maxima of the main branch of the spectrum were analyzed within LSW-theory Eqn. (2). The inspection of Fig. 3 reveals a strong in-chain dispersion and a much weaker one in the perpendicular $c$ and $a$ (not shown here) directions. The results of the fit are given in Table 1. The total width $W = \omega_{\pi/b} - \Delta = 2 \mid J_1 + J_3 + J_5 + \cdots - 0.5\left(\tilde{J}^{xy}_0 - D\right) \mid - \Delta \approx 2 \mid J_1 \mid$, i.e. the in-chain dispersion yields a direct measure of the NN coupling since $W$ is *un*affected by $J_2, J_4, J_6 \cdots$. Supposing a monotonous behaviour of $\omega_q$ up to the zone boundary at $Q = 0.5$ (corresponding to $q = \pi/b$), from the measured part of the full $\omega_q$-curve one obtains already a rigorous lower bound for $\mid J_1 \mid \gtrsim 150$ K. Our analysis shows that the in-chain NN interaction $J_1$ is strongly FM, but frustrated by an AFM NNN-coupling $J_2$ which affects the shape of $\omega_q$. In comparison, the AFM inter-chain coupling is weak, clearly demonstrating the magnetically quasi-1D character of the compound. For the in-chain coupling we find $\alpha = -J_2/J_1 = 0.33$, *unambigously above* the critical ratio $\alpha_{\rm crit} = 1/4$ for an isotropic Heisenberg-chain [26]. Note that the dispersion near the zone center behaves like $\omega(q) \propto q^4$ to be discussed below. We confirm also theoretical predictions [12, 14] (see also Tab. 1 for our results) that the main inter-chain coupling is indeed the NNN coupling along $(\frac{a}{2}, \frac{3b}{2}, \frac{c}{2})$. The NN inter-chain exchange has a negligible effect on the dispersion in the (0 $K$ $L$)-plane.

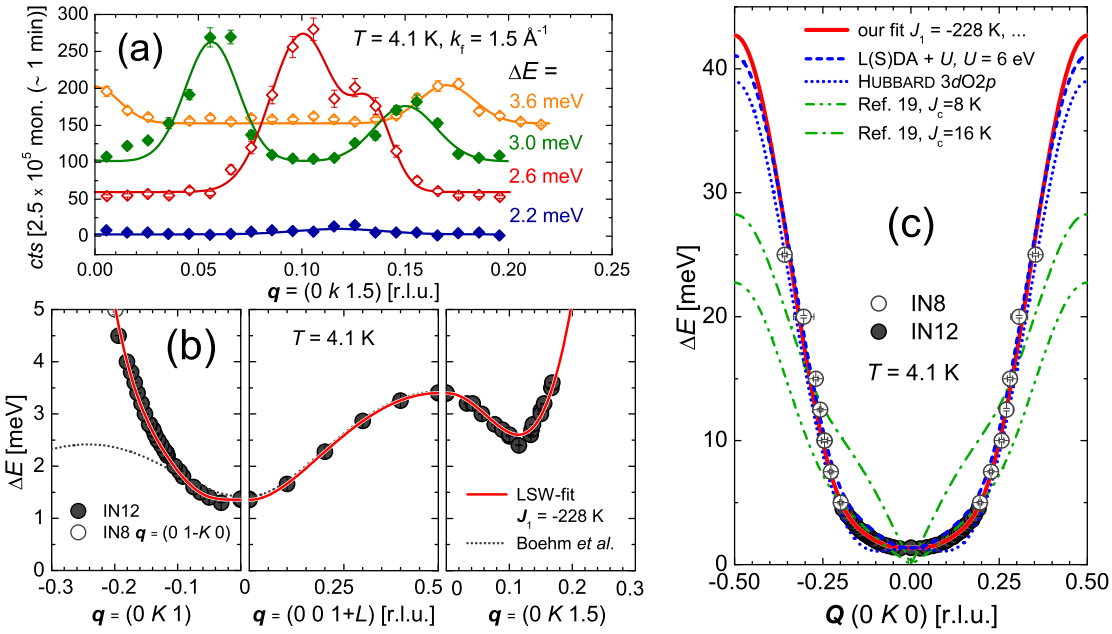


Figure 3: (Color online) (a)-Constant energy scans for the data points shown in part (b) (right panel) near the minimum. (b,c) - INS data points and LSW fits (red line) of the magnon dispersion (b): along $\vec{q}$ =(0 $K$ 1), (0 0 1 + $L$), (0 $K$ 1.5) for $E$-transfer below 5 meV, compared with Ref. [18] (black dotted line); (c) - along $Q$ = (0 $K$ 0) up to high $E$-transfer. Solid red line: our fit (see Tab. 1). For comparison the LSW dispersions predicted in Ref. [19] (green dashed-dotted and dashed double dotted lines), by our L(S)DA+$U$ (blue dashed line) calculation and the five-band Hubbard model (blue dotted line), both with the added experimental spin gap are shown, too.

Although further couplings can not be accessed from our fits, the main $J$ values given here do not change much, if the INS data are analyzed in more complex models with additional exchange paths, especially $J_3$ and $\tilde{J}_1$. When taken into account, both remain small ($\sim$ 4 K and 1 K, respectively) in full accord with L(S)DA+$U$ (see Tab. 1).

**4. DISCUSSION.** – The actual CC-AFM-FM ordering seemingly contradicts the IC "spiral" phase expected for a frustration ratio of $\alpha \approx 0.33$ in a 1D-approach (in the sense of the wave vector $q_0 \neq 0, \pi/b$ where the magnetic structure factor $S(q)$ becomes maximal [26]). Hence, the obtained relatively small but frustrated AFM inter-chain coupling may hinder the spiral formation. Thus, the 3D critical point compared with $\alpha_c^{1D}$ is upshifted:

$$\alpha_c^{3D,iso} = \alpha_c^{1D}\,(1 + \beta_1 + 9\beta_2 + 25\beta_3 + \cdots)\ , \qquad (5)$$

where $\beta_n = -\tilde{J}_n/J_1$. Eqn. (5) has been derived in the isotropic (iso) case [27]. Ignoring all other very weak inter-chain couplings $\tilde{J}_n$ we arrive with our results $\tilde{J}_2 = 9.04$ K and $J_1 = -228$ K at $\alpha_c^{3D,iso} = 0.339$. Anisotropies (aniso), as found here, further stabilize the CC-AFM-FM state. From Eqns. (2,3) we estimate finally $\alpha_c^{3D,aniso} \approx 0.39$. The combined effect of AFM inter-chain coupling and easy-axis anisotropy is also responsible for the anomalous $q^4$-dependence of the spin excitations mentioned above. In the limit $q_b b \to 0$ we expand Eqn. (2) and obtain

$$\omega(q) \approx \Delta + A_\Gamma (q_b b)^2 + B_\Gamma (q_b b)^4, \qquad (6)$$

$A_\Gamma$ and the quadratic dispersion vanish exactly at

$$\alpha_0^q = \frac{1}{4}\left(1 + \frac{9\beta_2}{\delta}\right) = 0.33098, \quad \delta = 1 - \frac{D}{4\tilde{J}_2}. \qquad (7)$$

Accidentally $Li_2CuO_2$ is very close to this point and its dispersion near the zone center is *quasi-quartic*. But in the presence of a spin gap $\Delta$ caused by the anisotropy $D$ this vanishing of the quadratic dispersion doesn't yet signal an instability of the CC-AFM-FM state.

Near the Z-point $(0, 0, \pi/c)$ the quadratic coefficient $A_Z$ is already essentially negative (see Fig. 3 (b, right panel)). Since along the line $Z - R(0, \pi/b, \pi/c)$ the inter-chain dispersion vanishes one can easily read off the 1D Fourier components of the exchange interactions $J_{\mathbf{q}}^{xy}$ (see Eqn. (4)). A similar rare situation occurs in the 2D frustrated $CsCuCl_4$ system in a high magnetic field above its saturation limit [28]. The clearly visible minima at $q_{b,0}b = \cos^{-1}(1/4\alpha) \approx \pm 0.72 = \pm 0.11$ (r.l.u.) correspond to the two equivalent propagation vectors of a low-lying spiral excitation [29] with a pitch angle of about 41.2° above a CC-AFM-FM ground state observed to the best of our knowledge for the first time.

Next, we briefly compare our results with those obtained so far by INS-studies for $Ca_2Y_2Cu_5O_{10}$ (CYCO) [17] with a similar FM in-chain ordering and a frustrating AFM inter-chain interaction. There the reported $J_1$ read -80 K and -93 K for fits where $J_2 = 0$ and $J_2 = 4.6$ K, respectively. However, such tiny values of $J_2$ are unlikely

Table 1: The fitted exchange integrals (in K) as determined from the INS data using Eqns. (2,3) compared with microscopic theory (see text) and other recent theoretical results. Values in parentheses are estimates from less accurate fits.

| | $J_1$ | $\alpha$ | $J_2 = -\alpha \cdot J_1$ | $J_3$ | $\tilde{J}_2$ | D | $\tilde{J}_1$ |
|---|---|---|---|---|---|---|---|
| INS / present work | $-228 \pm 5$ | $0.332 \pm 0.005$ | $76 \pm 2$ | (3.8) | $9.04 \pm 0.05$ | $-3.29 \pm 0.2$ | (1) |
| $3d$O2$p$ / present work [37]: | $-218$ | 0.30 | 66 | $-0.4$ | – | – | – |
| $3d$O2$p$ [30]: | $-143$ | 0.23 | 33 | $-1$ | – | – | – |
| $3d$O2$p$ [10]: | $-103$ | 0.47 | 49 | $-2$ | – | – | – |
| two-chain phenomenol. [19]: | $-100$ | 0.40 | 40 | – | 16 | – | 16 |
| LSDA+$U$, $U = 6$ eV [38]: | $-216 \pm 2$ | 0.31 | $66 \pm 2$ | $5 \pm 2$ | $13 \pm 2$ | – | 0±2 |
| GGA +$U$, $U = 6$ eV [14]: | $-171$ | 0.60 | 98 | – | 18 | – | 0.23 |
| RFPLO, LAPW+SO [40]: | – | – | – | – | – | $-15.6$ | – |

[10, 19, 30]. For a standard Cu-O hybridization a much larger value is expected [31] in accord with the observed sizable part of the total magnetic moment (22 % ) residing at O [32]. Re-fitting their INS data yields $J_1$,$J_2$ values of the same order as we found for $Li_2CuO_2$ (LCO) ($J_1^{\rm CYCO} \sim J_1^{\rm LCO}$ and $J_2^{\rm CYCO} \sim 0.5 J_2^{\rm LCO}$). A detailed comparison of both systems will be given elsewhere [31]. With respect to their large $J_1$ values the question may arise why they have been not recognised so far in analyzing thermodynamic properties? In this context a critical evaluation of the reported AFM "Curie-Weiss" (CW) temperatures $\Theta_{\rm CW}^{\rm CYCO} \approx -15$ K [33] or small FM values: 5-10 K [34] and $\Theta_{\rm CW}^{\rm LCO} \approx -40$ [8, 18] or -8 K [35] is very instructive. All these data have been derived from the linear fits of inverse susceptibility plots below 300–400 K (of the type denoted as "pseudo"-CW-lines in Fig. 5). But here we estimate

$$\Theta_{\rm CW} \approx \frac{1}{2}\left[\mid J_1 \mid -J_2 - \frac{z_{int-ch}}{2}\left(\tilde{J}_1 + \tilde{J}_2\right)\right] > +54 \text{ K},$$

where the inter-chain coordination number $z_{int-ch} = 4, 8$ for CYCO and LCO, respectively. Thus, we arrive at about 60 K and 58±4 K, respectively. The inspection of Fig. 4 clearly shows that very high $T$ [36], *far above* any available data would be required to extract $\Theta_{\rm CW}$ from $1/\chi(T)$-data. To satisfy the incorrect $\Theta_{\rm CW}$-values strongly underestimated $J_1$-values have been adopted in Refs. [10, 18, 33–35]. Even the $2^{nd}$ order of high $T$-series expansion (HTS) approaches the experimental curve only above 400 K. Hence, even more any attempt to detect even a Curie-law [10] near 300 K must fail. Our $J_1$-values for LCO and CYCO from INS-data provide support for the large value we found in $Li_2ZrCuO_4$ from thermodynamic properties [6] but puzzle the tiny value reported for $LiVCuO_4$ [5] with a similar Cu-O-Cu bond angle.

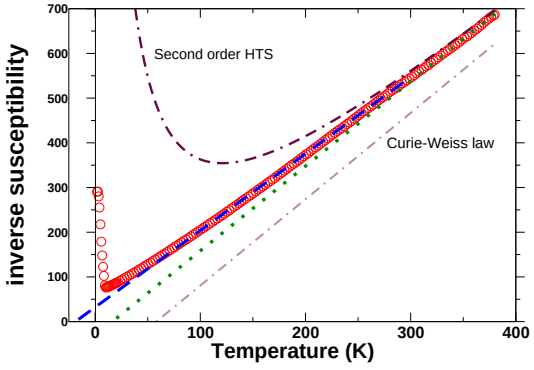


Figure 4: (Color online) The inverse spin susceptibility as measured (○) vs high $T$-series expansion in $1^{st}$ (correct CW-law) and $2^{nd}$ order. Dashed and dotted lines: "pseudo"-CW-laws.

Finally, we turn to a microscopic analysis. In Tab. 1 and Fig. 3 we compare our INS derived exchange integrals with theoretical results. First, we list the in-chain couplings $J_n$ as obtained from the mapping of a five-band extended Hubbard $pd$ model (on open chain $Cu_nO_{2n+2}$-clusters $n = 5, 6$) [37] on a corresponding $J_1$-$J_2$-$J_3$-Heisenberg model (see Fig. 1). But here, to reproduce the main experimental exchange integrals, a refinement has been performed most importantly by considering a larger direct FM Cu-O exchange $K_{pd} = 81$ meV compared with 50 meV adopted in Ref. [19]. We note that practically only $J_1$ is significantly affected by $K_{pd}$. Thereby $\mid J_1 \mid \propto K_{pd}$ holds approximately. Notice that the contribution of $K_{pd}$ is much more important for the large negative (FM) value of $J_1$ than that of the intra-atomic FM Hund's rule coupling on O. Since the available spectroscopic data at 300 K depend only weakly on $K_{pd}$ not much is known on its magnitude. In the past $K_{pd}$ has been used mostly as a fitting parameter for thermodynamic properties ranging from 50 to 110 meV for $CuGeO_3$ [10, 39]. The INS data reported here provide a unique way to restrict its value phenomenologically and opens a door for systematic studies of this very important interaction and well-founded comparisons with other edge-shared $CuO_2$ chain compounds.

Secondly, in the LSDA+$U$ there is practically only one adjustable parameter $U_d - J_H$, where $U_d$ denotes the Coulomb onsite repulsion (between 6 and 10 eV) and $J_H$ denotes the intra-atomic exchange ($\approx 1$ eV) both on Cu-sites. Comparing the total energy of various ordered magnetic states, a set of in-chain and inter-chain integrals can

be derived [14]. As a result one arrives again at very close numbers to our INS derived set [38]. Noteworthy, both ED a well as the LSDA+$U$ provides a justification to neglect any long-range exchange beyond the third NN. The latter also explains why there is only one important interchain exchange integral $\tilde{J}_2$ ($\beta_2$). The excellent agreement between the INS-data analyzed in the simple LSW-theory and the theoretical results/predictions suggests that in the present case the effect of quantum fluctuations as well as of spin-phonon interaction seems to be rather weak. The former point is also supported by the relatively large value of the magnetic moment $m \approx 0.96\mu_{\rm B}$ [8,9] in the ordered state below $T_N$ and a consequence of the fact that the FM state is an eigenstate of the 1D spin-model in contrast to the Néel state. Concerning the value of the anisotropy, there is no good agreement between contemporary DFT calculations [40] and much smaller values obtained in various experiments [18,24] including our data (see Tab. 1).

**5. SUMMARY.** – The main results of our INS study are (i) the relatively large dispersion of spin excitations in the $CuO_2$ chains of $Li_2CuO_2$ due to the large value of the FM NN in-chain coupling $J_1$ and (ii) the observation of a low-energy spiral excitation over a commensurate collinear Néel ground state in the vicinity of the 3D critical point above the corresponding 1D point. The obtained main exchange integrals can be approximately reproduced adopting an enhanced value for the direct FM exchange $K_{pd}$ between Cu $3d$ and O $2p$ states within an extended five-band Hubbard-model. Further support for the empirical exchange integrals comes from L(S)DA+$U$ calculations, if a moderate value of $U$ somewhat smaller than the $U_d$ in exact diagonalization for the extended Hubbard-model is employed. The achieved detailed knowledge of the main exchange couplings derived from the INS-data provides a good starting point for an improved general theoretical description of other $CuO_2$-chain systems and to adress a microscopic theory of their exchange anisotropy.

* * *

We thank the DFG [grants KL1824/2 (BB, RK & WEAL), DR269/3-1 (S-LD & JM), & the E.-Noether-progr. (HR)], the progr. PICS [contr. CNRS 4767, NASU 243 (ROK)], and ASCR(AVOZ10100520) (JM) for financial support as well as M. Boehm, M. Matsuda, A. Boris, H. Eschrig, V.Ya. Krivnov, D. Dmitriev, S. Nishimoto, E. Plekhanov and J. Richter for valuable discussions.

References

[1] Hoppe R. and Rieck H., *Z. anorg. allg. Chem.* , **379** (1970) 157 and references therein.
[2] Matsuda M.,*et al.,Phys. Rev. B* , **54** (1996) R15 626
[3] Matsuda M.,*et al.,Phys. Rev. B* , **63** (2001) 180403(R)
[4] Masuda T.,*et al.,Phys.Rev. B* , **72** (2005) 014405
[5] Enderle M.,*et al.,Europhys. Lett.*, **70** (2005) 337
[6] Drechsler S.-L.,*et al.,Phys.Rev.Lett.*, **98** (2007) 07202
[7] Drechsler S.-L., *et al. J.Phys.Cond.Mat.*, **19** (2007) 145230
[8] Sapiña F.,*et al., Solid State Commun.*, **74** (1990) 779
[9] Chung E., *et al. Phys. Rev. B* , **68** (2003) 144410.
[10] Mizuno Y.,*et al. Phys.Rev. B* , **57** (1998) 5326. The $J_n$ given in Tab. 1 in the $4^{th}$ row we have estimated in the same way as proposed in the present work and Ref. [30]. They slightly differ from those for a dimer and an artificial trimer (without the central Cu site) given by the authors.
[11] Weht R.,*et al.Phys. Rev. Lett.*, **81** (1998) 2502
[12] de Graaf C., *et al.,Phys. Rev. B* , **66** (2002) 014448
[13] Drechsler S.-L.,*et al.,J.Mag.Mag.Mat.*, **316** (2007) 306
[14] Xiang H. J.,*et al.,Phys.Rev. B* , **76** (2007) 220411(R). The $J$-values shown in Tab. 1 are linear interpolations between the values given for $U_{eff} = U - J_d = 4$ and 6 eV by the authors since in our calculation the standard value $J_d = 1$ eV for the Hund's rule coupling has been used.
[15] Dmitriev D.V.,*et al., Phys. Rev. B*, **77** (2008) 024401
[16] Plekhanov E., *et al. arXiv:*, (2008) 0811.2973v1
[17] Matsuda M.,*et al.Phys. Rev. B* , **71** (2005) 104414
[18] Boehm M., *et al. Europhys. Lett.* , **43** (1998) 77
[19] Mizuno Y., *et al. Phys. Rev. B* , **60** (1999) 6230 The relatively large dispersion in view of $J_1 = 100$ K, only, (shown in Fig. 4) results from an adopted significant interchain coupling (see Tab. 1) $\tilde{J}_1 = \tilde{J}_2 = 16$ K. Their sum strongly exceeds our empirical INS or L(S)DA+$U$- derived effective value by a factor of 3.5.
[20] Oguchi T., *Phys. Rev.* , **117** (1960) 117
[21] Behr G., *et al.,J. Cryst. Growth* , **310** (2008) 2268
[22] Ortega R.J.,*et al. J. Appl. Phys.*, **83** (1998) 6542
[23] Staub U., *et al. Physica B*, **289-290** (2000) 299.
[24] Ohta H., *et al.*, *J. Phys. Soc. Jpn.* , **62** (1993) 785
[25] Our notation coincides with that used in Ref. [2] but differs from that of Ref. [18]: we denote the interaction of a pair of spins $\hat{S}^{\alpha}_{\mathbf{m}}$ and $\hat{S}^{\alpha}_{\mathbf{m}+\mathbf{R}}$ as $J^{\alpha}_{\mathbf{R}}$. We use positive(negative) signs for AFM(FM) exchange, respectively.
[26] Bursill R., *J. Phys. Cond. Mat.* , **7** (1995) 8605
[27] Drechsler S.-L.,*et al. J.Mag.Mag.Mat.*, **290** (2005) 345
[28] Coldea R.,*et al. Phys.Rev.Lett.*, **88** (2002) 137203
[29] Kuzian R.O.,*et al.Phys. Rev. B*, **75** (2007) 024401
[30] Málek J., *et al. Phys. Rev. B* , **78** (2008) 060508(R)
[31] Kuzian R.O. , *et al. in preparation*, (2009)
[32] Matsuda M.,*et al. Appl.Phys.A*, **74[Suppl.]** (2002) S637
[33] Yamaguchi H.,*et al.,Physica C*, **320** (1999) 167
[34] Kudo K.,*et al. Phys. Rev. B*, **71** (2005) 104413
[35] Ebisu S., *et al.,J. Phys. Chem. Sol.* , **59** (1998) 1407
[36] $T > 1000 - 2000$ K, where the $2^{nd}$ order of the HTS approaches the Curie-Weiss line.
[37] Our parameters were adapted to describe optical, EELS and O $1s$ XAS-spectral data [30, 41] at 300 K. Careful measurements in the whole $T$-range down to 4 K as reported here for the INS would be very helpful for their further refinement, especially concerning the intersite Coulomb interactions $V_{pd}$, $V_{pp}$, and $V_{dd}$. But here and in Ref. [30] $V_{pd}$ etc. have been ignored for the sake of simplicity. A detailed discussion will be given elsewhere.
[38] Drechsler S.-L., *et al. J. Phys.: Conf.Ser.*, **145** (2009) 012060.
[39] Braden M., *et al. Phys. Rev. B*, **1996** (54) 1105
[40] D. Mertz,*et al.Phys. Rev. B*, **72** (2005) 085133
[41] Neudert R., *et al. Phys. Rev. B*, **60** (1999) 13413.